

Cite this: *Soft Matter*, 2011, **7**, 7382

www.rsc.org/softmatter

PAPER

# The porous nano-fibers raft: analysis of load-carrying mechanism and capacity

Abraham Marmur<sup>\*a</sup> and Robin H. A. Ras<sup>b</sup>

Received 29th January 2011, Accepted 24th May 2011

DOI: 10.1039/c1sm05156c

A simple model of a raft made of spaced nano-cylinders is formulated and discussed, in order to improve the understanding of load-carrying capacity of insects and miniature devices that float on liquids. It is shown that mostly the outer cylinders of the raft determine the load-carrying capacity. Therefore, the raft porosity (spacing of the cylinders) is instrumental mainly in increasing the load-carrying capacity per unit weight of the raft. In addition, it is shown that the actual contact angle that the liquid makes with the surface of a cylinder does not necessarily have to be higher than 90° in order to support a load; therefore, the raft may support a load both on water and on oil. Nonetheless, the load-carrying capacity and the floating stability increase when the contact angle increases.

## 1. Introduction

Flotation of objects at the interface between a liquid and a fluid (usually air) is ubiquitous in biology, industry, and daily life. Well-known examples include the water strider,<sup>1</sup> separation of valuable minerals from ores,<sup>2</sup> separation of pollutants in wastewater treatment,<sup>3</sup> and flotation of food powders on water prior to their complete wetting. The mechanism underlying flotation depends on the size of the object. Whereas large objects may float mainly due to buoyancy, surface tension comes into play when the object size is comparable or smaller than the capillary length (that is at the mm scale). The smaller the size of the object, the more meaningful becomes the effect of surface tension relative to weight and buoyancy.

Recently, attention has been drawn to the flotation of small objects on liquid surfaces that not only remain floating under their own weight, but in addition also have sufficient load-carrying capacity to support onboard cargo. Copper meshes,<sup>4,5</sup> carbon fiber fabrics,<sup>6</sup> cotton fabrics with silica nanoparticles,<sup>7</sup> silica aerogels,<sup>8</sup> and cellulose aerogels<sup>9</sup> have been suggested for applications concerning flotation on water surfaces. Furthermore, it has recently been demonstrated that properly treated nanocellulose aerogel membranes allow flotation and load carrying not only on water, but also on oil.<sup>9</sup> The above-mentioned porous materials differ in density of the solid constituent (to be referred to as “fiber”), its wettability, lateral size of the fiber (*e.g.* diameter), and pore size. For example, the copper mesh and cotton fabric have pore sizes in the tens or

hundreds of micrometres, while silica and cellulose aerogels have pore sizes in the tens or hundreds of nm range. It is therefore of much interest to understand the effects of the above parameters on the load-carrying capacity of the floating object. The objective of this paper is to theoretically study these effects using a simple model that consists of a raft made of spaced nano-cylinders.

## 2. Theory

As a first approximation, a nano-fibers raft can be modeled as a set of  $n$  parallel, infinitely long cylinders of radius  $R$  and density  $\rho_c$ . For simplicity, the cylinders are constrained to be all tangent to the same plane and at a fixed distance,  $2\beta R$ , between their centers (Fig. 1a). Since all the equations below refer to the two-dimensional geometry of infinitely long cylinders, the adjective “infinitely long” will be omitted in the following, for brevity. The raft floats on a liquid of density  $\rho_l$ , which is smaller than that of the fibers. Fig. 1a demonstrates a possible equilibrium position of the raft, where it is pushed to be under the level of the surface of the surrounding liquid by its own weight and by an applied load, while surface tension and buoyancy forces keep it from sinking (see Fig. 1b for a schematic of the forces on one cylinder). Fig. 1a also suggests, as will be explained in detail below, that the forces acting on the inner cylinders may be different in magnitude from those acting on the outer cylinders. In reality, the forces acting on a soft nano-fibers raft may cause it to bend or tilt, as, for example, in the case of non-uniform load distribution. In the present analysis, though, the raft is assumed to be flat, rigid, and horizontal, in order to capture the main physical picture by a relatively simple analysis.

The balance of forces that ensures equilibrium for a loaded mass floating on the surface of a liquid is  $F_{\text{load}} = F_{\text{surface tension}} - F_{\text{gravity}} + F_{\text{buoyancy}}$ . In the particular case of a single cylinder

<sup>a</sup>Department of Chemical Engineering, Technion—Israel Institute of Technology, 32000 Haifa, Israel. E-mail: marmur@technion.ac.il; Fax: +972-4-829-3088

<sup>b</sup>Department of Applied Physics, Aalto University (formerly Helsinki University of Technology), Puumiehenkuja 2, FIN-02150 Espoo, Finland

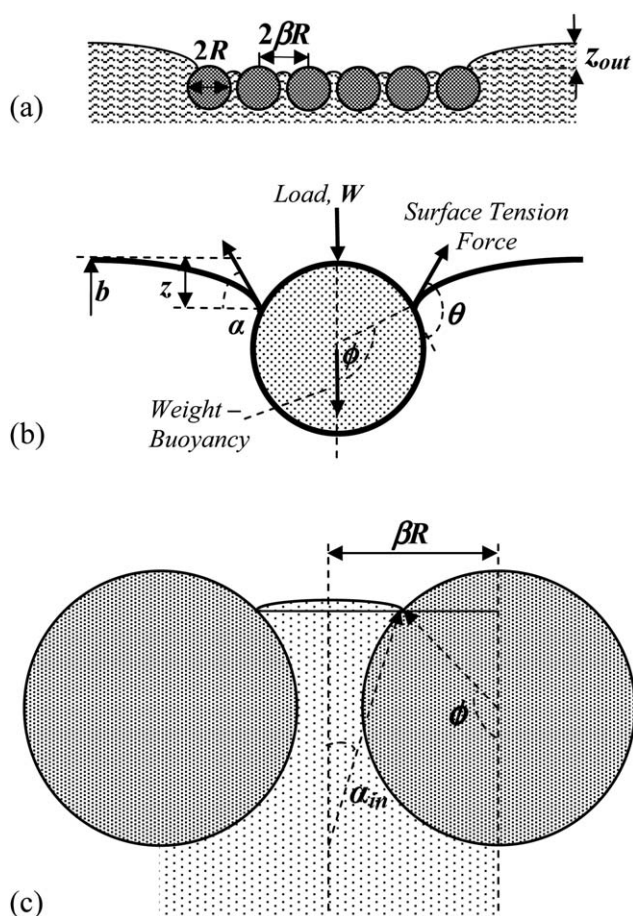


**Fig. 1** (a) A cross-section through the model cylinders-raft; (b) the forces acting on a cylinder and the geometrical definitions used in the force balance (eqn (1)); (c) the geometric presentation of the derivation of eqn (4) for  $\alpha_{in}$ .

floating on a liquid in ambient air atmosphere, the load-carrying capacity at equilibrium between the acting forces (see Fig. 1b) is given by

$$w = 2\sigma \sin \alpha - \pi R^2 \rho_c g + R^2 \rho_l g (\phi - \sin \phi \cos \phi) + 2(\sigma/b + z\rho_l g)R \sin \phi \quad (1)$$

In this equation,  $w$  is the load acting on the cylinder per unit of its length (positive when pointing downwards),  $\sigma$  is the surface tension of the liquid,  $\alpha$  is the angle between the surface tension force and the horizontal plane (positive when pointing upwards),  $g$  is the gravitational acceleration,  $\phi$  is the angle between the vertical direction and the radius that ends at the contact line between the cylinder and the liquid,  $z$  (positive when pointing downwards) is the depth of this contact line below the top of the liquid–air interface (meniscus), and  $b$  is the (positive) radius of curvature at the top of the meniscus. This curvature is zero ( $b \rightarrow \infty$ ) for a single cylinder and also for the external menisci of the outer cylinders of the raft, since they are far away from any other object. However, it is not zero when the meniscus is constrained by forced proximity of other cylinders, *e.g.* in-between the inner cylinders. Eqn (1), which is explained below in detail, is a straightforward generalization of the equilibrium equation for

an unloaded, floating cylinder,<sup>10,11</sup> adding the effects of the load and the curvature at the top point of the meniscus.

The first term on the right-hand side in eqn (1) expresses the vertical components of the surface tension forces per unit length acting on the cylinder at its two sides, assuming they are identical (which is true for an inner cylinder, and will be separately discussed for the outer cylinders). The second term describes the weight of the cylinder per unit length. The third term, where  $R^2(\phi - \sin \phi \cos \phi)$  is the volume per unit length of the submerged part of the cylinder, represents the buoyancy acting on the cylinder had the liquid–air interface at contact with the cylinder been flat, horizontal, and at the level of the surrounding liquid far away from the cylinder. In other words, this would have been the buoyancy force had the liquid pressure at the contact line been atmospheric. The fourth term adjusts the buoyancy force for the fact that the pressure in the liquid at the contact line is higher than atmospheric pressure by  $(\sigma/b + z\rho_l g)$ , acting on an effective area (between the two parallel triple lines on the opposite sides of the cylinder) per unit length of  $2R \sin \phi$ . The angles  $\alpha$  and  $\phi$  are related to  $\theta$ , the contact angle that the liquid makes with the cylinder surface (assuming it to be an ideal surface) by:

$$\alpha = \phi + \theta - \pi \quad (2)$$

An order of magnitude analysis is now applied to check the relative significance of the various terms in eqn (1), as they apply to a single nano-cylinder, for which  $R < 10^{-6}$  m. The first term on the right-hand side of eqn (1), which is independent of  $R$ , is of the order of magnitude  $10^{-1} \sin \alpha$  N m<sup>-1</sup>. The value of  $\alpha$  at maximum load will be  $\sim \pi/2$  (maximum of  $\sin \alpha$ ), so the first term in this case is of the order of magnitude of  $10^{-1}$  N m<sup>-1</sup>. The second and third terms contain  $R^2$  and must be smaller than  $10^{-7}$  N m<sup>-1</sup>, since  $R^2 (< 10^{-12}$  m<sup>2</sup>) is multiplied by a factor that is of the order of magnitude of  $10^4$  to  $10^5$  N m<sup>-3</sup>. For estimating the fourth term, it is required to evaluate  $z_{out}$  ( $b \rightarrow \infty$  in this case), where the subscript *out* indicates the outer menisci. The value of  $z_{out}$  is well known<sup>8,11</sup> to be  $\sqrt{2\sigma(1 - \cos \alpha)/(\rho_l g)}$ , thus its highest possible value is the capillary length  $a \equiv \sqrt{2\sigma/(\rho_l g)}$ . This value is  $\sim 3.8$  mm for water, and lower for organic liquids. Thus, the order of magnitude of the fourth term is smaller than  $10^{-4}$  N m<sup>-1</sup>. The above analysis then leads to the simple conclusion that the effect of all gravity-related terms is negligible for a single nano-cylinder. The load-carrying capacity is determined to a very good approximation by the surface tension forces alone. Since the two outer menisci of the raft act together like the two menisci of a single nano-cylinder, the load-carrying capacity of these menisci is

$$w_{out} = 2\sigma \sin \alpha_{out} \quad (3)$$

The state of the inner cylinders is different from that of the outer ones. Because of the assumed rigidity of the raft, their depth under the free surface of the liquid is fixed to be the same as that of the outer cylinders, and the distance between them is *a priori* fixed. The liquid meniscus in-between inner cylinders must have at its apex a curvature ( $1/b$ ) that conforms to the hydrostatic pressure of the liquid inside the meniscus. The value of  $b$  is estimated as follows. The contact lines of the outer menisci are at a depth of  $z_{out}$  under the free surface of the liquid, which is

of the order of magnitude of  $10^{-3}$  m when the maximum load is applied. The radius of the nano-cylinders is by a few orders of magnitude smaller than  $z_{\text{out}}$ . Therefore, the contact lines of the inner menisci, as well as their apexes, are, to an excellent approximation, at a depth of  $z_{\text{out}}$  below the free surface of the liquid far away from the raft. Consequently, the pressure difference across the meniscus in-between the inner cylinders is very well approximated by the hydrostatic pressure difference,  $z_{\text{out}}\rho_l g$ . This pressure difference that is imposed by the equilibrium position of the outer cylinders must be compensated for by the curvature of the meniscus in-between the cylinders. Therefore, according to the Young–Laplace equation,  $\sigma/b = z_{\text{out}}\rho_l g$ . From this equation it is clear that  $b$  is of the order of magnitude of at least  $10^{-2}$  m. The fourth term on the right-hand side of eqn (1) is then smaller than  $10^{-4} \sin \phi \text{ N m}^{-1}$ , similarly to the case of the outer menisci. Since at maximum load the nano-cylinders may be almost completely immersed in the liquid, the value of  $\phi$  may be close to  $\pi$ , thus the fourth term may even be of the order of magnitude of  $10^{-5} \text{ N m}^{-1}$  or less. The third and second terms are also similar to the case of the outer menisci. However, the first term is different because of the value of  $\alpha$ .

To estimate  $\alpha_{\text{in}}$ , where the subscript *in* indicates the internal menisci, it is necessary to realize that  $b$  is orders of magnitude larger than  $R$ . Consequently, the meniscus between the inner cylinders is rather flat, and can be approximately described by a large circle. As can be seen in Fig. 1c,  $\alpha_{\text{in}}$  can be very well estimated from eqn (2) and the simple geometrical relationship  $\beta R = b \sin \alpha_{\text{in}} + R \sin(\pi - \phi)$  as

$$\sin \alpha_{\text{in}} \approx (\beta - \sin \theta)R/b \quad (4)$$

In this equation it is *a priori* assumed that  $\alpha_{\text{in}}$  is much smaller than  $\theta$ , which is true because  $b$  is very large.  $R/b$ , as discussed above, is of the order of magnitude of  $10^{-4}$ , and it is reasonable to assume that  $\beta$  is of the order of magnitude of 1. Thus,  $\sin \alpha_{\text{in}}$  may be as small as  $10^{-4}$ , and the first term on the right-hand side of eqn (1) is of the order of magnitude of  $10^{-5} \text{ N m}^{-1}$ .

### 3. Results and discussion

As mentioned in the introduction, the various small, floating, load-carrying devices proposed in the literature differ in density, lateral size and wettability of the fibers, and in their porosity. It is clear from the above analysis that, as the fiber radius gets smaller, a bigger share of the force needed to support the external load comes from surface tension. Thus, the fiber radius should be as small as practically possible, *i.e.* it is preferable to use nano-fibers ( $R < 10^{-6}$  m). Another advantage of using nano-fibers is, as shown by the above order of magnitude analysis, that the effect of fiber density is negligible for this size range of fibers. In order to understand the advantages of the porous raft that consists of spaced nano-cylinders it is important to realize the mechanism of load carrying by the raft and compare it with a non-porous one. This is done in the following paragraphs. Then, the effect of wettability will be discussed.

The above analysis indicates that the load-carrying capacity of an inner nano-cylinder may be smaller by about three or four orders of magnitude than that of the outer ones. However, the

number of inner nano-cylinders is, of course, much bigger than that of the outer ones. This number can be estimated by

$$n = \frac{L + 2(\beta - 1)R}{2\beta R} \approx \frac{L}{2\beta R} \quad (5)$$

where  $L$  is the width of the raft. Assuming  $L$  to be of the order of magnitude of  $10^{-2}$  m, the number of nano-cylinders may be bigger than an order of magnitude of  $10^3$ . Thus, the overall contribution of all the inner nano-cylinders may be roughly similar in order of magnitude to that of the two outer ones.

In the extreme case of a non-porous raft, in which the cylinders touch each other, the main upward force on the inner nano-cylinders is the additional buoyancy stemming from the fact that the raft is forced to be at a depth of  $z_{\text{out}}$  under the free surface of the liquid. The contribution to the carried load of the inner nano-cylinders in this case is the pressure difference times the width (which stands for area per unit length):

$$F_{\text{up}} \approx L\rho_l g z_{\text{out}} \quad (6)$$

where  $F_{\text{up}}$  is the upward force acting on the inner nano-cylinders of the non-porous raft (in addition to the surface tension forces on the outer cylinders). This force is of the order of magnitude of  $10^{-1} \text{ N m}^{-1}$ , which is similar to the one predicted for the spaced inner nano-cylinders. Thus, the load-carrying capacity is not very sensitive to the spacing of the nano-cylinders. This result *a posteriori* justifies the simplification of the theoretical model by assuming a fixed distance between the cylinders.

However, the load-carrying capacity per unit weight of the raft may be much higher in the case of the porous raft. Therefore, the main contribution of introducing porosity appears to be to increase the load-carrying capacity per unit weight of the raft. This conclusion cannot, of course, be taken to imply that the number of inner fibers should approach zero. For specific cases, it may be possible to perform a detailed optimization of the size and porosity of the raft, to get the best load-carrying capacity per unit weight while retaining the necessary raft size and mechanical strength.

Next, it is important to understand the effect of  $z_{\text{out}}$ , the raft position relative to the free liquid surface, on the stability of the raft. Similarly to the stability analysis done long ago for a single, floating particle,<sup>11</sup> the raft loses its stability when the vertical force balance on the outer cylinders cannot prevent them from

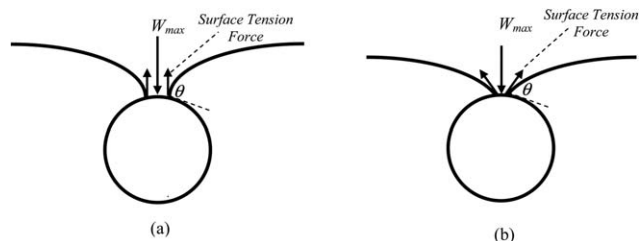


**Fig. 2** (a) The maximum load for the case of  $\theta > 90^\circ$  is achieved when the surface tension force points vertically upwards (meniscus is pointing vertically downwards); (b) the maximum load for the case of  $\theta < 90^\circ$  is achieved when the meniscus gets almost to uppermost line on the cylinder (surface tension force is pointing upwards at the maximum possible angle).

sinking into the liquid. One of two criteria, depending on which of them is first fulfilled, can be used to define the stability limit. One possible limit (see Fig. 2a) is  $\alpha = \pi/2$  (that corresponds to  $z_{\text{out}} = a \equiv \sqrt{2\sigma/(\rho_l g)}$ ), since then the load-carrying capacity is maximal,  $w_{\text{out}} = 2\sigma$ . From a mathematical point of view there could be an equilibrium depth of the contact line at  $z_{\text{out}} > a$ ; however, the contact line cannot be stable at  $z_{\text{out}} > a$ . This is so, since at  $z_{\text{out}} > a$  the angle  $\alpha$  must be  $>\pi/2$  ( $\sin \alpha < 1$ ), and the equilibrium load is smaller than its maximum. Thus, once the maximum possible load is applied, any further push on the cylinder beyond  $z_{\text{out}} = a$ , whatever its magnitude, will cause it to sink. The other possible stability limit (see Fig. 2b) is  $\phi = \pi$ , because then the two liquid–air interfaces meet and the cylinder is wrapped by the liquid. Since by eqn (2)  $\alpha = \phi + \theta - \pi$ , the latter stability applies for  $\theta < \pi/2$ , because  $\phi$  will reach  $\pi$  before  $\alpha$  will reach  $\pi/2$  ( $\alpha \leq \theta$  in this case). The former stability limit applies for  $\theta > \pi/2$ , because then  $\alpha$  will reach  $\pi/2$  before  $\phi$  reaches  $\pi$ .

It is important and interesting to notice that, as has been known for a long time,<sup>11</sup> it is not necessary to have an obtuse contact angle,  $\theta > \pi/2$ , in order to keep a (nano-)cylinder floating. As explained above, even if  $\alpha < \theta < \pi/2$ ,  $\sin \alpha$  is still positive and can support a load. The theoretical upper limit for the load when the contact angle is acute, defined by  $\phi = \pi$ , is  $2\sigma \sin \theta$ . The maximum possible load carried by the outer nano-cylinders is decreased, for example, only by a factor of 2 when the contact angle is brought down from  $\pi/2$  to  $\pi/6$ . However, the system will be practically less stable than for  $\theta > \pi/2$ , since the maximum load is achieved when the two external contact lines on the outer nano-cylinders get to the top of the nano-cylinders and the liquid may completely wrap the cylinders.

Some experimental evidence for the present analysis can be achieved by measuring the maximum depth of the contact line of the outer nano-cylinders. As mentioned above, this depth, for a single nano-cylinder, is given by  $a \equiv \sqrt{2\sigma/(\rho_l g)}$ . This expression can be applied to the outer nano-cylinders, so

$$\max\{z_{\text{out}}\} = \begin{cases} a & \text{if } \theta > \pi/2 \\ a\sqrt{1 - \cos \alpha} = a\sqrt{1 - \cos \theta} & \text{if } \theta < \pi/2 \text{ and } \phi = \pi \end{cases} \quad (7)$$

For water,  $a \approx 3.8$  mm, and for a liquid of lower surface tension that still gives  $\theta > \pi/2$  it will be  $\sim 3.8\sqrt{(\sigma/\sigma_w)(\rho_w/\rho_l)}$  mm, where the subscript  $W$  indicates properties of water. If  $\theta < \pi/2$ , the contact angle with the solid material from which the cylinder is made must be known. Assuming an extreme case of  $\theta = \pi/3$ , for example, the maximum depth will be about 71% of the value of  $a$ . Indeed, the experimentally measured depth for water was 3.7 mm, and that for paraffin oil ( $\sigma = 32.9$  mN m<sup>-1</sup>) was 2.7 mm, in agreement with the above estimates.<sup>9</sup> In addition, the calculated load per unit mass can be compared with some experimental indications. Using eqn (3) and (5), one gets that this ratio can be as high as the order of magnitude of  $10^3$ , quite similar to the experimentally observed ratio.<sup>9</sup>

## 4. Conclusions

An order of magnitude analysis of a floating nano-cylinders raft and its load-carrying capacity leads to the following conclusions:

(1) The flotation of nano-cylinders is dominated by surface tension forces, and is practically independent of gravity-related forces.

(2) Much (sometimes most) of the load is carried by the outer cylinders of the raft. The inner cylinders altogether carry a load that may be similar in order of magnitude to the load carried by the two outer cylinders.

(3) The main function of the inner cylinders is to prevent penetration of the liquid through the raft.

(4) In order to keep the raft floating, the surface tension of fibers does not have to be associated with contact angles higher than 90°. However, the floating stability and load-carrying capacity improve when the contact angle increases.

(5) The major advantage of the porosity of the raft is to increase the ratio of the load to the weight of the raft itself, compared with a raft of non-porous bottom.

## Acknowledgements

This research was supported by Finnish National Technology Agency (TEKES), UPM-Kymmene, Nokia, Ahlstrom, Ecopulp, Glykos, Elastopoli, Sinebrychoff, Kareline, Dynea, and Teknos within the NASEVA project.

## References

- P. J. Wei, S. C. Chen and J. F. Lin, *Langmuir*, 2009, **25**, 1526; Z.-g. Zhou and Z.-w. Liu, *J. Bionic Eng.*, 2009, **6**, 1; P. P. Goodwyn, E. De Souza, K. Fujisaki and S. Gorb, *Acta Biomater.*, 2008, **4**, 766; X.-Q. Feng, X. Gao, Z. Wu, L. Jiang and Q.-S. Zheng, *Langmuir*, 2007, **23**, 4892; F. Shi, J. Niu, J. Liu, F. Liu, Z. Wang, X.-Q. Feng and X. Zhang, *Adv. Mater.*, 2007, **19**, 2257; J. W. M. Bush and D. L. Hu, *Annu. Rev. Fluid Mech.*, 2006, **38**, 339; X. Gao and L. Jiang, *Nature*, 2004, **432**, 36.
- B. A. Wills, *Mineral Processing Technology*, Pergamon Books Inc., Elmsford, NY, 1988.
- J. Rubio, M. L. Souza and R. W. Smith, *Miner. Eng.*, 2002, **15**, 139.
- Q. M. Pan and M. Wang, *ACS Appl. Mater. Interfaces*, 2009, **1**, 420.
- Z. X. Jiang, L. Geng and Y. D. Huang, *J. Phys. Chem. C*, 2010, **114**, 9370.
- Z. X. Jiang, L. Geng and Y. D. Huang, *Mater. Lett.*, 2010, **64**, 2441.
- Y. Zhao, Y. W. Tang, X. G. Wang and T. Lin, *Appl. Surf. Sci.*, 2010, **256**, 6736.
- N. Hüsing and U. Schubert, *Angew. Chem., Int. Ed.*, 1998, **37**, 22.
- H. Jin, M. Kettunen, A. Laiho, H. Pynnönen, J. Paltakari, A. Marmur, O. Ikkala and R. H. A. Ras, *Langmuir*, 2011, **27**, 1930; J. T. Korhonen, M. Kettunen, R. H. A. Ras and O. Ikkala, *ACS Appl. Mater. Interfaces*, 2011, **3**, 1813.
- H. M. Princen and S. G. Mason, *J. Colloid Interface Sci.*, 1965, **20**, 246.
- H. M. Princen, *Surface And Colloid Science*, ed. E. Matijevic, Wiley-Interscience, vol. 2, 1969, pp. 1–84.